

Evaluation of biosorption potential of *Gracilaria corticata* for the removal of malachite green from aqueous solution: isotherm, kinetic and thermodynamic studies

M. Jerold, K. Vasantharaj, C. Vigneshwaran, V. Sivasubramanian*

Department of Chemical Engineering, National Institute of Technology Calicut, Kozhikode – 673 601, Kerala, India, Tel: +91-4952285406; Fax: +91-4952287250; email: siva@nitc.ac.in; Tel. +91-9486252374; emails: jerold88@gmail.com (M. Jerold), kvasantharaj@gmail.com (K. Vasantharaj), vignesh.vij@gmail.com (C. Vigneshwaran)

Received 9 April 2016; Accepted 28 June 2016

ABSTRACT

In the present study, the protonated *Gracilaria corticata* (PGC) biomass has been successfully used as biosorbent for the removal of malachite green (MG) from aqueous solution. The biosorbent was characterized by scanning electron microscopy (SEM), Fourier transform infrared spectroscopy (FTIR), elemental analysis, pHpzc, and Boehm titration, respectively. The degree of MG biosorption was investigated as a function of pH, adsorption time, biosorbent concentration, initial dye concentration, agitation rate and temperature. The maximum biosorption of MG was observed at the biosorbent concentration of 0.1 g/L, initial pH 10, temperature 30°C, agitation rate 150 rpm, and initial dye concentration of 100 mg/L. Various isotherm models were used to evaluate the equilibrium data obtained. The equilibrium data best fitted with Langmuir model with highest coefficient of determination 0.994. The Langmuir monolayer biosorption capacity was recorded as 100 mg/g. In addition, study of RL, the dimensionless factor revealed the favorability of the isotherm. The kinetic data were well described using pseudo-second-order kinetic model. Thermodynamic profile indicated the biosorption of MG is favorable and spontaneous in nature. The reusability of the PGC biomass was investigated using 0.1 M HCl. Attempts were also made to study the continuous biosorption in up-flow packed bed column. Overall, the present study proved that, PGC biomass can be effectively used as biosorbent for the removal of MG bearing wastewater.

Keywords: Biosorption; Algae; Malachite green; Wastewater; SEM; FTIR; Isotherms; Kinetics

1. Introduction

Today, control of pollution has become a major concern among the society. There are various reasons by which water gets polluted. One among them is pollution by the release of dyes and dye stuffs from various process industries. Several industries make use of dye which includes textile, leather, cosmetics, printing, paper, pharmaceuticals, food processing, and so on to add color to their products. Textile dye is rated as the utmost dye stuffs produced which records two third of the total outcome of the dye stuffs [1,2]. The effluents released from these industries will be

moreover partially treated or untreated wastewater may perhaps create a severe problem to the environment [3]. About two third of the total dye stuff produced is utilized alone in textile industries and 10%–15% released out as effluent. These dye contaminants affect the aesthetic value of water system by imparting the color in the receiving streams. Color mainly interferes the penetration of sunlight into water which retards the photosynthesis and in turn inhibits the growth of aquatic species [4]. Harmful carcinogenic metabolite products derived from dye stuffs which have mutagenic, carcinogenic and teratogenic effects. Furthermore, the release of such waste contaminated water into municipal water plants results in the development of serious diseases among the public. The ETDA (Ecological

*Corresponding author.

and Toxicological Association of the dyestuff) survey has reported that 90% of the dye stuffs have LD50 values greater than 200 mg/kg. Among these dyes, basic and diazo direct groups are identified to have high rates of toxicity [5].

Malachite green (MG) is a N-methylated diamino-triphenylmethane dye most widely used for coloring purposes among all dyes [6,7]. It has a wide application in cotton, wool, paper, silk, leather, jute, and distillery industries. The basic cationic dyes are used as therapeutic agent (fungicide, ectoparasiticide) and as antiseptic. Oral consumption is restricted because of the toxicity and carcinogenicity but can be used as external agents for healing of wounds and ulcers. The release of such a harmful pollutant into the streams will have deleterious effect on aquatic life. In humans, MG causes respiratory tract irritation and gastrointestinal tract if ingested. Various other diseases caused by MG in humans are skin irritation, eye injuries, tumor and so on. Even though, MG has toxicological effects, still they are used in aquaculture and other industries.

The Central Pollution Control Board (CPCB), New Delhi, India, has developed Minimum National Standards (MINAS) for various manufacturing industries. According to the standards, the release of colored product is not permitted. Hence, the decolorization of the effluents has become mandatory before their discharge into land. There are various physical and chemical methods for the treatment of dye laden waste water namely flocculation, electro-floatation, precipitation, electro-kinetic coagulation, ion exchange, membrane filtration, electrochemical destruction, irradiation, ozonation and so on [4]. However, these methods have been failed due to high capital cost and less effectiveness. Adsorption technique has widely accepted method for the treatment of dye bearing effluent because of ease of operation, less cost, simple design, less sensitivity to toxicological substances. Activated carbon is the successfully implemented adsorbent for the adsorption process because of greater surface area, enhanced adsorption capacity and so on [8–11]. But the application has been limited due to its high cost [12]. This lead the researchers to search for cheaper substituting material. Several agro wastes have been used for the biosorption process such as wheat straw [13,14] durain peel [15], rice husk [16], orange peels [17]. In addition to the agro wastes, a number of biosorbents including bacteria [18], fungi [19], yeast [20] and algae [21,22] have been utilized. Algal biosorption has gained attention due to their significant adsorption behavior. Particularly, marine algae have been chosen by several authors to treat the metal/dye bearing wastewater due to various advantages such as high mechanical stability, macroscopic structure, low cost and variety of binding groups [23,24]. *G. corticata* possesses unlimited amount of chemical groups such as carboxyl, sulphonate, hydroxyl and amino groups which is the salient feature of this kind of seaweed. Thus, in the present investigation, *G. corticata* marine red alga is selected as a biosorbent for the removal of basic cationic dye, MG from aqueous solution. The main objective of the study was to evaluate the biosorption potential of *G. corticata* as a function of various operating conditions such as pH, initial dye concentrations, agitation and biosorbent dosage. The equilibrium and kinetic data were described using different isotherm and kinetic models. The morphological features of the biosorbent were characterized by various analytical techniques.

2. Materials and methods

2.1. Reagents and chemicals

MG dye was purchased from Nice Chemicals, India. The dye is used in the form of oxalate form is commercial grade with 70 % purity. All other chemicals were purchased locally with at least 98% purity and used without any further purifications. All solutions were prepared using distilled water.

2.2. Preparation of biosorbent

Gracilaria corticata, a red marine alga, was collected in Mandapam, Tamilnadu, India. It was washed with running tap water and then sun dried. The fine dried biomass was ground to an average particle size of 0.7–1.0 mm and then protonated using 0.1 M HCl for 3–4 h. The biomass was washed with distilled water to remove the excess of HCl and dried at 60°C in hot air oven overnight. The dried algal biomass was subsequently used for the biosorption experiment.

2.3. Dye solution and determination of dye concentration

MG is a basic cationic dye of triphenylmethane group. Stock solution of the dye was prepared and diluted to various concentrations with distilled water. The solution pH was adjusted with 1 mol/L of NaOH or HCl. A standard calibration curve was generated by measuring the absorbance at 617 nm.

2.4. Characterization of biosorbent

2.4.1. SEM, FTIR and CHNS analysis

The surface morphology of the biosorbent was visualized using the scanning electron microscopy (SEM) (JSM-6390LV, JEOL, USA) which shows the changes in the surface texture before and after biosorption of dye. Fourier transform infrared spectroscopy (FTIR) reveals the involvement of functional groups in the biosorption of dye. Therefore, spectra of PGC before and after biosorption were collected 500–4,000 cm^{-1} using FTIR spectrophotometer (Nicolet Avatar 370, Thermo Scientific, India). Furthermore, to know the percentage of elements C, H, N and S in the protonated *Gracilaria corticata* (PGC), biomass was analyzed using C-H-N-S Analyzer (Vario EL III, Elementar, Germany).

2.4.2. Determination of point of zero charge (pHpzc)

The point of zero charge characteristics of PGC biomass was checked out in an array of Erlenmeyer flask of 250 mL capacity. In each of the flask, 100 mL of 0.01 N KMnO_3 solutions were transferred. A different solution pH of 3 to 10 was prepared by using 0.1 M HCl and 0.1 M NaOH and it is designated as pH0. To each of the flask, 0.1 g of respective adsorbents was added and agitated for 48 h at room temperature. After the contact time, the final pH of the samples was analyzed. The difference between the initial and final pH values ($\Delta\text{pH} = \text{pH}_0 - \text{pH}_f$) was plotted against the pH0, and the point of intersection of the curve at which ΔpH is zero gave the pH_{PZC}.

2.4.3. Boehm titration

The PGC biomass was characterized using Boehm titration method [25] to study the amount of functional groups present. 500 mg of PGC biomass was transferred to 250 mL flask containing each containing 100 mL of 0.05 M NaHCO₃, 0.05 M Na₂CO₃, 0.05 M NaOH and 0.05 M HCl. Each of the flasks was agitated for 24 h at room temperature. After 24 h, the supernatant was separated and titrated against 0.1 M NaOH or 0.1 M HCl depending on the initial salt solution used. The amount of functional groups was calculated based on the assumptions that: NaHCO₃ neutralizes only carboxylic groups, Na₂CO₃ neutralizes carboxylic and lactonic groups, and NaOH neutralizes carboxylic, lactonic and phenolic groups, while HCl neutralizes basic groups [26].

2.5. Batch biosorption experiment

Biosorption of MG using PGC biomass was studied by performing a batch experiment in an Erlenmeyer flask of 250 mL with 100 mL of dye solution and agitating in a rotary incubatory shaker (OSI-24C; Labline, India). The various operation parameters such as pH, contact time, biomass dosage, agitation rate, temperature, initial dye concentration were determined for the removal of MG from aqueous solution. The supernatant was removed and subsequently used for the analysis of residual dye content using double beam UV-visible spectrophotometer (2201; Systronics, India) at 617 nm. The amount of dye adsorbed by PGC biomass at equilibrium, q_e (mg/g) was calculated using the following equation:

$$q_e = \frac{(C_0 - C_e)V}{M} \quad (1)$$

where V is the solution volume (L), M is the mass of the biosorbent (g) and C_0 and C_e are the initial and equilibrium dye concentrations, respectively.

The rate of biosorption was calculated by conducting a batch experiment in an Erlenmeyer. PGC Biomass was added to the solution at different concentrations (20 mg/L to mg/L) of MG dye and the samples were withdrawn at periodic time intervals and subsequently analyzed for the dye concentration. The dye uptake at time t , q_t (mg/g), was estimated using the mass balance,

$$q_t = \frac{(C_0 - C_t)V}{M} \quad (2)$$

2.6. Desorption and regeneration studies

The reusability of biosorbent with efficient elution of adsorbate is an important for any potential application of a biosorbent. To assess the biosorption capacity of spent biosorbent, the MG laden PGC biomass was subjected to the consecutive biosorption-desorption process. A maximum of three cycles of biosorption-desorption process was carried out. The spent PGC biomass was regenerated using 0.1 M HCl, where dye laden PGC biomass was agitated

at 150 rpm, 30°C in Erlenmeyer flask containing 100 mL of 0.1 M HCl for 60 min. The supernatant was subjected to U-V analysis and the dye uptake was determined.

2.7. Column studies

The column study was carried out to investigate the practical application of biosorption process. The continuous flow experiment was conducted in packed bed glass column with an *id* 1.5 cm and 20 cm in length. A layer of glass beads was placed at the bottom of the column to provide uniform inlet flow of dye solution into the column. Followed by the glass beads, a 0.5-mm glass wool serves as the supporting bed for the resting of the PGC biomass. A dye solution (pH 10) of 5 mg/L was fed into the column with a flow rate of 10 mL/min using a peristaltic pump (Rivotek-50171 002; Riveria, India). The effluents were collected at different fractional volume and subjected to the U-V analysis using double beam UV-visible spectrophotometer (2201; Systronics, India) at 617 nm. The operation was stopped when the effluent concentration exceeded a value of 99.5 mg/L or higher.

3. Results and discussion

3.1. Characterization of biosorbent

3.1.1. SEM analysis

SEM images of PGC before and after biosorption are shown in Fig. 1. The PGC biomass without contact with dye solution is more fibrous and compact with various macroporous surface as shown in Fig. 1(a). However, after contact with dye, the pores on the surface of PGC biomass vanished due to the occupation of the adsorbate into the pores [27] and cavities filled with the dye as shown in Fig. 1(b), which further allows the diffusion of the dye into the various pores of the PGC biomass. Therefore, after biosorption, a smooth morphology was observed in the PGC biomass (Fig. 1(b)). A similar kind of observation was made during the biosorption of MG onto brown seaweed and epicarp of *Ricinus communis* [21,28].

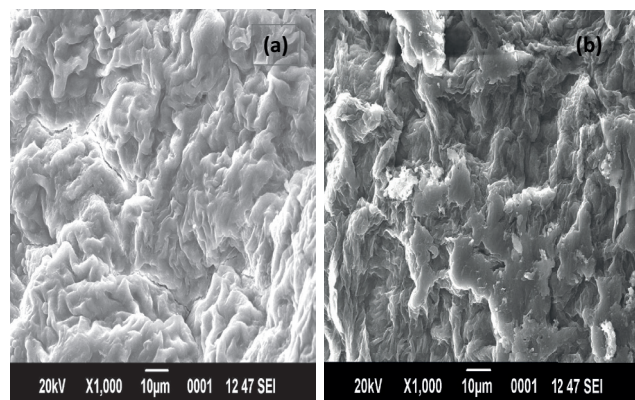


Fig. 1. Scanning electron microscopy images of PGC biomass (a) before MG biosorption and (b) after MG biosorption.

3.1.2. FTIR analysis

FTIR technique was used to examine the surface functional groups of PGC biosorbent and to identify the functional groups responsible for the biosorption [29]. Therefore, the dye-free PGC biomass and dye-laden PGC biomass were subjected to FTIR analysis and the spectra was recorded in the range between 4,000 and 500 cm^{-1} . Fig. 2(a) shows the FTIR vibrational spectra before biosorption and Fig. 2(b) shows the FTIR vibrational spectra after biosorption. The resultant peaks at 3,415.03 cm^{-1} are assigned to OH-bond stretching in the dye loaded PGC biomass (Fig. 2(a)). The other absorption bands 2,939.24 cm^{-1} ; 1,637.72 cm^{-1} ; 1,075.80 cm^{-1} ; 632.23 cm^{-1} indicated the presence of CH₂, C=O, C-O and C-H groups. Among these, OH-bond and CH₂ group play an important role in the biosorption of MG. PGC biomass is very special class of biosorbent and has an array of functional groups on the surface. These functional groups bear surplus active sites. These functional groups are available in the form of amino acids. The PGC is red algal biomass, which contains starch and polysaccharides. These polymeric carbohydrate molecules are composed of long chains of monosaccharide units bound together by glycosidic linkages. Thus, PGC biomass seems to possess heterogeneous class of functional group over the surface which helps in the mission of biosorption of the malachite dye. The polarities of the groups also tend to influence the sorption process [30]. In the present study, the biomass is protonated in order to remove the irrelevant ions present in the biomass. Hence, there will not be any hindrance during the dye biosorption. This enables good binding of the adsorbate to the active binding groups in the biosorbent [31].

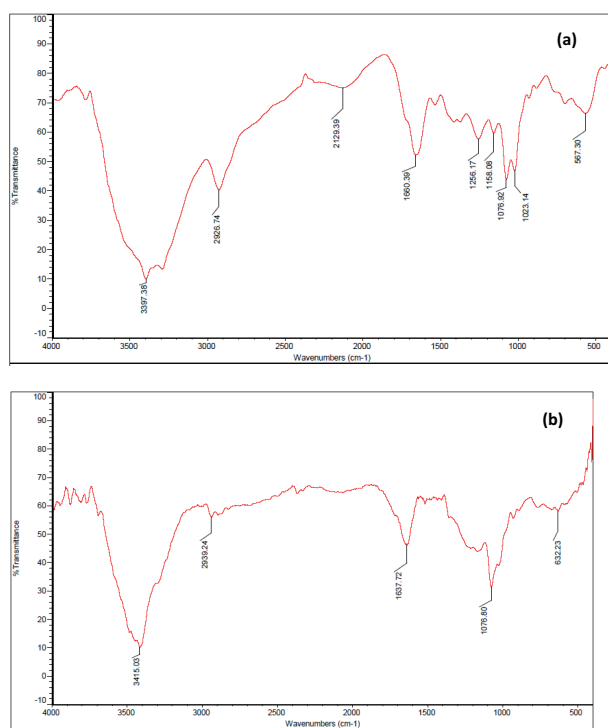


Fig. 2. (a) FTIR spectra of PGC biomass and (b) FTIR spectra of dye-laden PGC biomass.

3.1.3. CHNS analysis

Generally, the red marine alga contains sulfated polysaccharide carrageenan in the amorphous sections the cell wall. These carrageenan molecules made up of repeating galactose units and 3,6 anhydrogalactose (3,6-AG), both sulfated and nonsulfated. The units are joined by alternating α -1,3 and β -1,4 glycosidic linkages. The biosorbent PGC used in the present study is red algae (Rhodophyceae). From the CHNS analysis, it was observed that the PGC biomass was rich with carbon molecules. Table 1 shows the amount of carbon and other elements present in the PGC biomass. From Table 1, it was confirmed that PGC has a complex mixture of functional groups in the biomolecules, which facilitate a better binding for the biosorption dyes.

3.1.4. Point of zero charge

The charge over the surface of the PGC biomass was determined through Point of zero charge methodology. It gives an idea that at which pH value the charge of acidic and basic groups are equal. Fig. 3 shows the pHPZC plot for PGC biomass. From the plot, it was found that the PGC had a pHPZC value of 7.01, indicating the excessive presence of acidic groups on the biosorbent. Therefore, when the solution pH is greater than 7.01, the PGC biomass surface becomes more negatively charged, and favors the biosorption of cationic MG due to the electrostatic force of interaction. Hence, in the present study, the solution pH was adjusted above the pHPZC value. A similar kind of result was reported in biosorption of MG using pomelo (*Citrus grandis*) peels [32].

Table 1
Elemental analysis of PGC biomass

Element	Percentage (%)
C	36.48
H	6.34
N	1.87
S	1.82

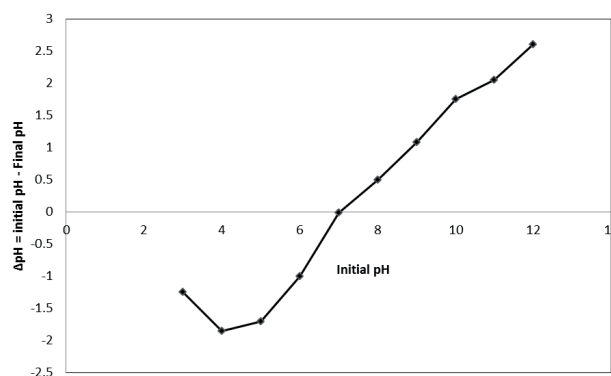


Fig. 3. The determination of the point of zero charge (pH_{PZC}).

3.1.5. Functional group analysis

The PGC surface chemistry was characterized through Boehm titration method and found that acid sites were predominantly occurs on the surface of the biomass with 17.61 mg/g. On the other hand, only 0.525 mg/g of basic site was observed on the PGC biomass. It shows that acidic functional sites were found to play a significant role in the biosorption of MG. Carboxylic ($-\text{COOH}$) which is found to be involved in the sorption process. Also, the titration results are in agreement with pHPZC. Thus, PGC biomass seems to possess infinite number of carboxylic groups from the carbohydrate molecules.

3.2. Effect of pH

pH is a very important factor in the adsorption process especially for dye biosorption [33]. The Initial experiments pertaining to the effect of equilibrium pH on MG removal revealed that alkaline conditions found to be most excellent for the maximum and effective removal of MG from aqueous solution. At alkaline condition, the positive charge at the solution interface decreases and the adsorbent surface appears negative. According to the above theory, at pH 10.0, there was maximum MG uptake of 66 mg/g as shown in Fig. 4. Solution pH influenced both carbon surface dye binding sites and dye chemistry in water. Hence, when the pH of the solution is decreased, there is a reduction in the dye uptake. At lower pH values, the carbon will have a net positive charge because at lower pH, the protonation occur on the cell wall of the biomass, that is, formation of positive charged ions (H^+) which competes with cationic dye; therefore, the sorption of dye is decreased [24].

3.3. Effect of biosorbent dosage

The effect of biosorbent dosage on the removal of MG by PGC biomass at initial concentration of 100 mg/L is shown in Fig. 5. It was observed that as biosorbent concentration increased, there was a negative influence in the uptake of the dye. The biosorption capacity of the PGC biomass decreased from 66 to 9.45 mg/g for MG due to increase in biosorbent dosage from 0.1 to 1.0 g/L. At higher biosorbent concentration, the sorbate species compete the occupation of active sites available in the PGC biomass. This phenomenon can be explained on the basis of splitting effect. The splitting effect exerted a flux (concentration gradient) between the sorbent and sorbate [34]. Nevertheless, the percentage of dye removal was found to increase. It was due to the rapid superficial adsorption accomplishment put forth onto the PGC biomass [35,36].

3.4. Effect of initial dye concentration and contact time

Generally, the initial dye concentration influences the biosorption process. Therefore, the effect of initial dye concentration on MG biosorption was investigated by varying the dye concentration between 20 to 100 mg/L. A plot of dye uptake q versus time t at various initial dye concentrations is shown in Fig. 6. The biosorption capacity was found to increase with an increase in the initial dye

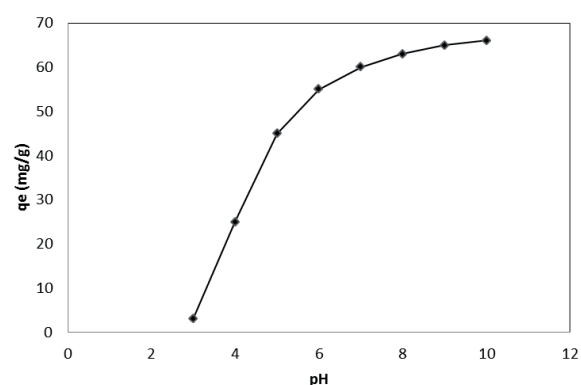


Fig. 4. Effect of pH (V: 100 mL; C_0 : 100 mg/L; M: 0.1 g; Temp: 30°C).

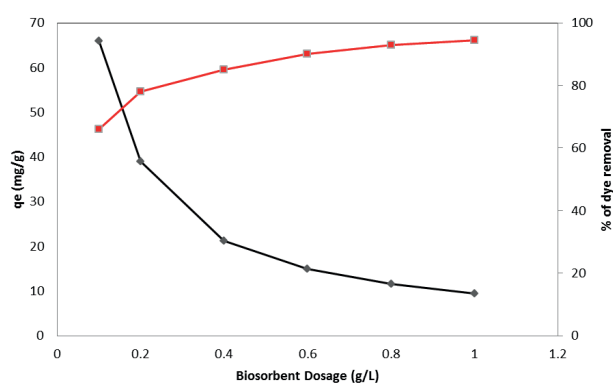


Fig. 5. Effect of biomass loading (V: 100 mL; C_0 : 100 mg/L; Temp: 30°C; pH: 10).

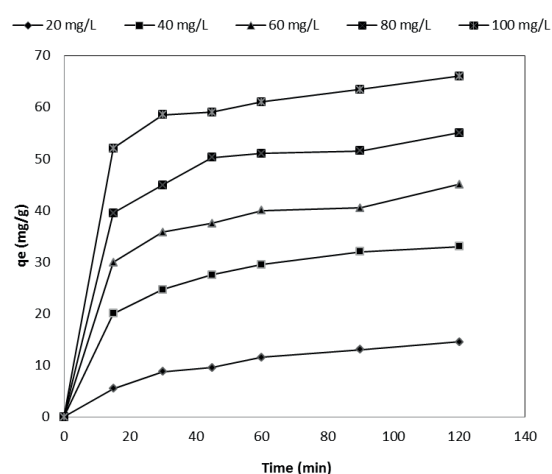


Fig. 6. Biosorption kinetics for malachite green PGC biomass (V: 100 mL; M: 0.1 g/100 mL; Temp: 30°C; pH: 10.0).

concentration; perhaps it was due to an increase in the driving force between the adsorbate-adsorbent. At earlier stage, surplus amount of active binding sites are available in the PGC biomass. This serves as the ground factor for the increased biosorption capacity. Also, the uptake was rapid

at the external surface of the PGC biomass and later the sorbate diffuse into the pores by an internal diffusion which is the rate controlling step. Due to the excess of MG ions, repulsion found to occur that results in the prolongation of equilibrium time [19]. Therefore, maximum initial dye concentration will possess larger ions, thus have a greater competition for the active sites present on the PGC biosorbent, and lead to the larger biosorption capacity.

3.5. Effect of agitation

In the batch biosorption systems, agitation plays a significant role in the biosorption process by affecting the external boundary film layer and inhibiting the distribution of the solute molecules in the bulk liquid phase. Hence, the effect of agitation was studied by varying the agitation speed from 50 to 200 rpm using 1 g/L of biosorbent and 100 mL of 100 mg/L of dye solution at pH 10.0. An uptake of 14.5 mg/g was recorded at a lower agitation of 50 rpm. However, when the agitation speed was increased from 50 rpm to 150 rpm, there was a substantial amplification in the biosorption capacity of the dye from 14.5 to 66.5 mg/g, respectively, as shown in Fig. 7. There is couple of reasons for the increase in biosorption of dye at higher agitation: (1) rapid migration of adsorbate molecules from the bulk solution to the surface of the adsorbent; (2) migration followed by intraparticle diffusion into the interior pores of the adsorbent. Due to the increase in turbulence, the rate of diffusion of dye molecules from bulk liquid to the liquid boundary layer surrounding the particle becomes higher and decreased thickness of the liquid boundary layer. In addition, the external sorption kinetic control plays a significant role [37]. However, further increase in agitation resulted in the decrease of biosorption capacity. It is due to the collision of sorbate molecules which enhanced the desorption tendency of dye. Thus, higher agitation resulted in elevated shear force which attributed in the breakage of bond between MG and PGC biomass [19].

3.6. Biosorption isotherm

The biosorption isotherm indicates the distribution of adsorption molecules between the solid and liquid phase when the sorption system is at equilibrium state. The selec-

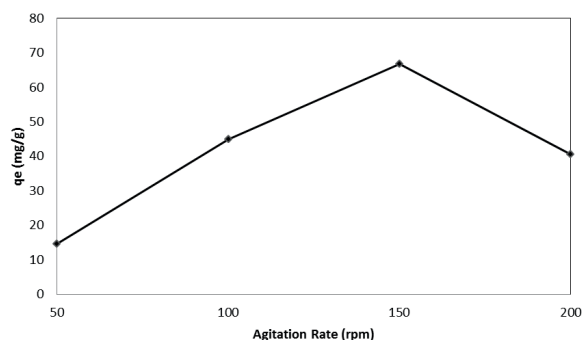


Fig. 7. Effect of agitation rate on biosorption of malachite green by PGC biomass (V: 100 mL; M: 0.1 g/100 mL; Temp: 30°C; pH: 10.0).

tion of suitable isotherm model for the design of adsorption system is basic criterion in the biosorption isotherm. This is accomplished by the data analysis in which the experimental isothermal data are fitted to different isotherm models [38]. It gives an idea about the interaction of solute with biosorbents.

In the present investigation, three different isothermal models were used to study the biosorption process namely Langmuir, Freundlich, and Temkin isotherm models [39]. The R^2 was taken into account for predicting the applicability of the isotherm model for the biosorption of MG onto PGC biomass.

3.6.1. Langmuir model

Langmuir model [40] is described based on the assumption that accumulation of saturated monolayer on the surface of the biosorbent corresponds to the maximum biosorption, and there is no further interaction between the adsorbed species. The Langmuir model is expressed by the following equation:

$$q_e = \frac{K_L q_{\max} C_e}{1 + K_L C_e} \quad (3)$$

where, q_e (mg/g) is the amount of dye adsorbed per unit mass of the biosorbent and C_e (mg/L) is the unadsorbed dye concentration in solution at equilibrium, q_{\max} is maximum amount of dye adsorbed per unit mass of the biosorbent in order to form solute monolayer on the surface of algal biomass at an equilibrium concentration, and K_L is a binding affinity constant related to the affinity towards the sorbate (L/mg). The linearized form of Langmuir isotherm equation is as follows:

$$\frac{1}{q_e} = \frac{1}{K_L q_{\max}} \left(\frac{1}{C_e} \right) + \frac{1}{q_{\max}} \quad (4)$$

If the plot of specific adsorption ($1/q_e$) against the equilibrium concentration ($1/C_e$) is linear, then it is concluded that particular adsorption system obeys the Langmuir model. The Langmuir constants q_{\max} and K_L were determined from the slope and intercept of the plot and are presented in Table 2.

The most essential characteristics of the Langmuir isotherm can be described in terms of a dimensionless Langmuir separation factor R_L and is presented in the following equation [41].

$$R_L = \frac{1}{(1 + K_L C_0)} \quad (5)$$

where C_0 is the maximum initial concentration of adsorbate (mg/L), and K_L (L/mg) is Langmuir constant.

The separation factor R_L can be described on the shape of isotherm either unfavorable ($R_L > 1$), linear ($R_L = 1$), favorable ($0 < R_L < 1$), or irreversible ($R_L = 0$). In the case of favorable isotherm, the R_L values are between 0 and 1. In the present study, biosorption of MG onto PGC biomass, the R_L value was found to be 0.246 (Table 3). Therefore, the adsorption is favorable.

Table 2
Langmuir, Freundlich, and Temkin isotherm model constants and correlation coefficients for adsorption of MG onto PGC biomass

Isotherm	Parameters
Langmuir	
q_{\max}	100.00
K_L	0.0306
R^2	0.994
RMSE	3.745
Freundlich	
K_F	4.375
n	1.414
R^2	0.986
RMSE	2.226
Temkin	
A	0.305
B	22.21
R^2	0.919
RMSE	3.456

3.6.2. Freundlich isotherm

Freundlich isotherm [42] is an empirical relation assumes heterogeneous adsorption due to the diversified distribution of adsorption sites on the surface of the biosorbent. The Freundlich equation is expressed as follows:

$$q_e = K_F C_e^{1/n} \quad (6)$$

From the Freundlich equation, K_F (mg/g) is the biosorption capacity of the sorbent and n represents the biosorption favorability. The Freundlich isotherm model is used to determine deducible constants. The degree of exponent, $1/n$ describes the favorability of biosorption process. Suppose, $n > 1$, then it naturally reflects that adsorption is favorable. A plot of $\ln(q_e)$ against $\ln(C_e)$ derived from linearized Freundlich equation is used to determine the constant values K_F and $1/n$.

$$\ln q_e = \ln K_F + \frac{1}{n} \ln C_e \quad (7)$$

From the slope and intercept values of the plot, n and K_F are calculated and tabulated in Table 2.

3.6.3. Temkin isotherm

Temkin and Pyzhev described the interaction between the adsorbate and adsorbent interactions on adsorption isotherms. It assumes that the heat of adsorption decreases linearly on a surface [43] and the molecules adsorbed over the surface is epitomized with consistent binding energies

Table 3
Langmuir separation factor for PGC biomass

Initial MG dye concentration (mg/L)	R_L
20	0.620
40	0.449
60	0.352
80	0.290
100	0.246

up to a notable maximum value. As a result, Temkin and Pyzhev suggested that due to the effect of indirect interaction of sorbate molecules, there is a significant reduction in the heat of adsorption of the sorbate on the surface of the adsorbent. The general Temkin isotherm is presented as follows:

$$q_e = \left(\frac{RT}{b} \right) (\ln C_e) \quad (8)$$

Eq. (8) is linearized and written as follows:

$$q_e = B \ln A + B \ln C_e \quad (9)$$

where $B = RT/b$, b is the Temkin constant related to heat of sorption (J/mol); A is the Temkin isotherm constant (L/g), R the universal gas constant (8.314 J/mol K) and T the absolute temperature (K).

Therefore, by plotting q_e versus $\ln C_e$ the constants A and B are determined and the constants A and B are listed in Table 2.

The experimental data were analyzed using Langmuir, Freundlich, and Temkin isotherms. Langmuir isotherm model was found to fit well with the experimental data obtained from biosorption of MG onto PGC biomass due to larger R^2 value of 0.994 as shown in Table 2. It confirms the experimental data into Langmuir isotherm equation. Hence, it indicates the homogeneous nature of PGC biomass surface, that is, each dye molecule/PGC biomass adsorption had equal binding energy. The maximum Langmuir biosorption capacity was found to be 100.00 mg/g. The results also demonstrated the formation of monolayer coverage of MG on the surface of PGC biomass. Table 4 compares the biosorption capacity of different types of adsorbent used for removal of MG. The value of q_{\max} in this study is larger than those in most of previous works. This suggests that MG could be easily adsorbed on surface of PGC biomass.

3.7. Biosorption kinetics

In biosorption process, kinetic study plays an important role in the design of an appropriate sorption treatment system [52,53]. It predicts the minimum time required for the uptake of dye on to the surface of the biosorbent from an aqueous solution. Therefore, it enables to determine the residence time of the biosorption process. In the present study, pseudo-first-order and second-order kinetic models are adopted to examine the mechanism of the biosorption process [54]. It is written as follows:

Table 4
Comparison of biosorption capacities of various adsorbents for Malachite Green

Adsorbents	q_{\max} (mg/g)	T (°C)	Reference
PGC biomass	100.00	30	This study
Treated ginger waste	84.03	30	[44]
Raw <i>S. swartzii</i> biomass	76.92	30	[21]
<i>Turbinaria conoides</i>	66.6	30	[45]
Rattan saw dust	62.71	30	[46]
Lemon Peel	51.73	32	[47]
<i>Caulerpa racemosa</i>	25.67	30	[48]
<i>Saccharomyces cerevisiae</i>	17	35	[49]
<i>Arundo donax</i> root carbon	9.35	40	[50]
Tamarind fruit shell	1.95	30	[51]

$$\frac{dq_t}{dt} = k_1(q_e - q_t) \quad (10)$$

Integrating this for the boundary conditions from $t = 0$ to $t = t$ and from $q_t = 0$ to $q_t = q_t$, gives the following equation:

$$\log(q_e - q_t) = \frac{\log q_e - k_1 t}{2.303} \quad (11)$$

where k_1 is the rate constant (1/h), q_e the solute uptake on the biosorbent surface at equilibrium (mg/g), q_t the amount of solute adsorbed at any time (mg/g). A plot of $\log(q_e - q_t)$ versus t gives the value of the biosorption rate constant (k_1) for MG sorption by PGC biomass. The pseudo-first-order model parameters are summarized in Table 5. Generally, Lagergren's first-order equation is not relevant to the whole period of adsorption process. However, it is only applicable in the initial stage of biosorption process. In the present study, the R^2 values obtained were comparatively small and the experimental q_e values were not predicted from the linear plots (Table 5). Therefore, it is suggested that the biosorption of MG on PGC biomass is not likely to follow the pseudo-first-order at initial MG concentrations as examined [55].

The next model used for the kinetic data analysis is the pseudo-second-order model. The equation is written based on equilibrium adsorption [56] and is expressed as follows:

$$\frac{t}{q_t} = \frac{1}{k_2 q_e^2} + \frac{t}{q_e} \quad (12)$$

where (q_e) equilibrium adsorption capacity and k_2 (g/mg h). The second-order rate constant can be determined from the plot of t/q_t versus t . The values of k_2 and q_e were computed from the model and are presented with their respective

Table 5
Kinetic parameters for the MG biosorption onto PGC biomass

Kinetic model	Parameters
Pseudo-first-order	
K_1 (1/min)	0.0276
$q_{e,cal}$ (mg/g)	64.60
R^2	0.922
RMSE	0.384
Pseudo-second-order	
K_2 (g/mg min)	0.0042
h (mg/(g min))	18.86
$q_{e,cal}$ (mg/g)	66.67
R^2	0.997
RMSE	0.481
Intraparticle diffusion	
K_{id} (mg/g h ^{1/2})	5.473
C	16.81
R^2	0.752
External diffusion	
K_{ext} (1/min)	0.002
R^2	0.912

coefficient of determination in Table 5. Table 5 indicates the applicability of this model to describe the adsorption process of MG onto PGC biomass.

In pseudo-second-order model, it is assumed that the sorption capacity is proportional to the number of active sites occupied on the sorbent; hence the kinetic rate law [56] can be written as Eq. (13):

$$\frac{t}{q_t} = \frac{1}{h} + t \left(\frac{1}{q_e} \right) \quad (13)$$

where $h = k_2 / q_e^2$. The values $1/h$ and q_e can be determined from the intercept and slope, respectively, from a linear plot of t/q_t and time.

Weber and Morris proposed a model based on the intraparticle diffusion theory [57]. It was used to describe the diffusion mechanism in the biosorption process. It can be written as follows:

$$q_t = K_{id} t^{1/2} + C \quad (14)$$

where C and K_{id} are intercept and the intraparticle diffusion rate constant (mg/g h^{1/2}), respectively, which can be evaluated from the plot q_t versus $t^{1/2}$ and the corresponding values are listed in Table 5. The boundary layer effect explains the rate controlling steps. The intercept of the plot represents the boundary layer effect. Larger the intercept, greater the contribution of the surface sorption in the rate

controlling step. If the plot of q_t versus $t^{1/2}$ is linear and the regression of the line passes through the origin, one can say that rate-limiting step is governed by intraparticle diffusion. However, in the present study at various concentrations, an absolute linearity was not obtained hence they did not pass through the origin. This clearly illustrated that the intraparticle diffusion was not only the sole rate controlling step. It may be due to the differences in the mass transfer in the initial and final stages of adsorption process.

The external diffusion model or boundary model [58] is based on the assumption that the solute concentration is negligible at time, $t = 0$ and as a result, the intraparticle diffusion is negligible. The external diffusion model can be written as follows:

$$\ln \frac{C_t}{C_0} = -k_{ext} t \quad (15)$$

A plot of $\ln(C_t)$ versus time gives a linear relationship for external diffusion model from which the model parameters are calculated and presented in Table 3.

From Table 5, it is observed that the experimental data fitted well with pseudo-second-order model when compared with pseudo-first-order model, intraparticle diffusion model and external diffusion model (boundary model). Hence, the pseudo-second-order model better represented the adsorption kinetics.

3.8. Thermodynamic studies

The thermodynamic study is based on the assumption that in an isolated system, energy cannot be lost or gained, where change in entropy acts as the driving force [59]. The Gibbs free energy change is related to the equilibrium constant for biosorption of MG onto PGC biomass and is expressed as follows:

$$\Delta G^\circ = -RT \ln K_c \quad (16)$$

where G° is the standard free energy change (J mol^{-1}), T the absolute temperature (K) and R gas constant ($\text{J mol}^{-1} \text{K}^{-1}$), K (L g^{-1}) an equilibrium constant (K_c) obtained by multiplying the Langmuir constants q_m and K_L .

Vant Hoff's equation gives a general relation between the standard enthalpy change and standard entropy change which is expressed as follows:

$$\ln K_c = \frac{-\Delta H^\circ}{RT} + \frac{\Delta S^\circ}{R} \quad (17)$$

where K_c is equilibrium constant for sorption, R gas constant ($\text{J mol}^{-1} \text{K}^{-1}$), T temperature (K). The value of ΔH° was calculated from the slope of the linear regression of $\ln K_c$ versus $1/T$. The K_c value was determined by the relation given as follows:

$$K_c = \frac{q_e}{C_e} \quad (18)$$

where q_e denotes the quantity of MG adsorbed on PGC biomass at equilibrium (mg/L), C_e is the MG in solution at equilibrium concentration (mg/L).

Table 6

Thermodynamic parameters of PGC biomass at different temperature

Temp. (K)	K_c	ΔG° (kJ/mol)	ΔH° (kJ/mol)	ΔS° (kJ/mol/K)
303	1.639	-1,246.23		
313	2.333	-2,205.17		
323	3.073	-3,015.44	25,557.23	88.541
333	4.128	-3,925.85		

The various thermodynamic parameters obtained for the biosorption of MG by PGC biomass are given in Table 6. The negative value of ΔG° indicates the feasibility of the sorption process and the spontaneous nature of the biosorption of MG onto PGC biomass. Hence, it confirmed the affinity of PGC biomass for MG sorption. The positive value of ΔH° implied that the adsorption phenomenon is endothermic in nature. The ΔS° is positive and revealed that there is an increase in randomness at the solid-liquid interface during the sorption of MG onto the surface of PGC biomass.

3.9. Regeneration studies

In the biosorption technology, regeneration and recycle of the spent biosorbent are most important and advantageous to reduce the cost for the large scale operation. Desorption process can be used for the regeneration of the exhausted biosorbent. From Fig. 4, it is observed that acidic condition was unfavorable for the biosorption of MG on PGC biomass. Therefore, acidic treatment can be used for the efficient desorbing agent for the successive usage of biomass. PGC biomass was effectively utilized for the biosorption of MG. From this study, it was observed that the biosorption capacity of PGC biomass tends to decrease after each cycle of operation viz. 57.72 mg/g, 53.56 mg/g and 47.5 mg/g, respectively. However, there was only a small decrease in the biosorption capacity. Thus, it is understood that APC biomass has good biosorption capacity due to the presence of large number of functional groups which are safely preserved in the PGC biomass. Hence, the acid treatment eliminates the sorbates and other metal ions and creates vacancy of active binding sites in the biomass surface.

3.10. Column studies

The process parameters were optimized from batch experiments and proved that PGC biomass has an excellent biosorption capacity. Therefore, the same biosorbent was used in a fixed-bed column to treat the MG bearing wastewater for continuous operation (Fig. 8). The breakthrough curve while passing the MG dye solution through the PGC biomass is shown in Fig. 9. Due to the accumulation of MG ions in the PGC biomass, there is no vacant space for occupying the adsorbate molecules. Therefore, both the outlet and inlet concentrations are consistent. Hence, no more biosorption is possible on to the PGC biomass. Thus, it was re-utilized after the successful regeneration process. In the

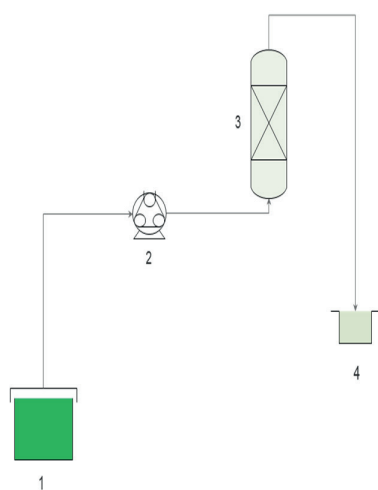


Fig. 8. Experimental set up of Fixed Bed Column for the biosorption of MG using PGC biomass: 1 – Influent MG solution; 2 – Peristaltic Pump; 3 – PGC fixed bed Glass column; 4 – MG Effluent.

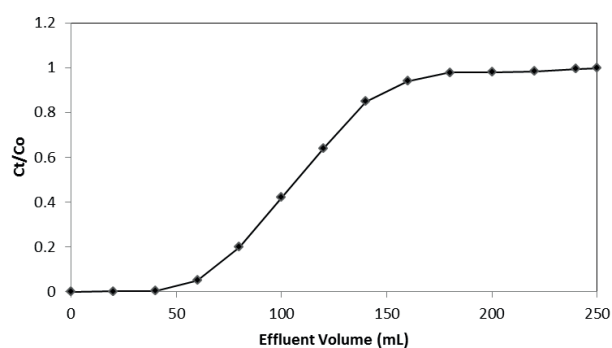


Fig. 9. Breakthrough curve for biosorption of MG in packed bed column by PGC biomass.

present study, ~60 mL of aqueous dye solution was treated in a fixed bed column packed with PGC biomass. Thus, PGC biomass can be effectively used as biosorbent for the treatment of aqueous MG bearing wastewater.

4. Conclusion

The biosorption capacity of PGC biomass for the removal of cationic dye MG from the aqueous solution was analyzed in the present investigation. The removal of MG by PGC biomass was classically optimized and investigated under different process conditions. Equilibrium results were well correlated with Langmuir isotherm in comparison with other isotherm models. The pseudo-second-order model was found to fit well with dynamic adsorption behavior. The thermodynamic parameters such as ΔH , ΔG and ΔS showed that the biosorption of MG ions onto PGC biomass was spontaneous, endothermic and increased randomness under the present experimental conditions. The regenerated PGC biomass has an appreciable dye uptake capacity. The dried PGC biomass was shown to have a fine mechanical

stability, flow permeability and MG uptake capacity in column operations. Therefore, the present study proved that PGC biomass has an excellent dye removal capacity. Hence, PGC biomass can be used as a promising biosorbent for the removal of MG from aqueous phase.

Symbols

A	—	Temkin isotherm constant, L/g
B	—	Temkin isotherm constant, L/g
b	—	Temkin constant related to heat of sorption, J/mol
C	—	Intercept
C_0	—	Maximum initial concentration of adsorbate, mg/L, initial dye concentration, mg/L
C_e	—	Dye concentration at equilibrium, mg/L
ΔG°	—	Gibb's free energy
ΔH°	—	Enthalpy change
K_F	—	Adsorption capacity of the sorbent mg/g, L/mg
K_{id}	—	Intraparticle diffusion rate constant, mg/g h ^{1/2}
K_L	—	Langmuir constant related the binding site affinity towards the sorbate, L/mg
M	—	Mass of the biosorbent, g/L
k_2	—	Second-order constants, g/mg h
n	—	Represents the favorability of the adsorption process
q_{max}	—	Maximum dye uptake per unit mass of the biosorbent to form monolayer, mg/g
q_e	—	Equilibrium adsorption capacity, mg/g
q_t	—	Dye uptake at different time, mg/g
R	—	Gas constant, 8.314 J/mol K
R_L	—	Langmuir separation factor
ΔS°	—	Entropy change
T	—	Adsorption temperature, K
V	—	Volume of dye solution, mL

References

- [1] S.S. Azhar, A.G. Liew, D. Suhardy, K.F. Hafiz, M.D.I. Hatim, Dye removal from aqueous solution by using adsorption on treated sugarcane bagasse, *J. Appl. Sci.*, 2 (2005) 1499–1503.
- [2] V.K. Garg, R. Kumar, R. Gupta, Removal of malachite green dye from aqueous solution by adsorption using agro-industry waste: a case study of *Prosopis cineraria*, *Dyes Pigments*, 62 (2004) 1–10.
- [3] B.D. Bhole, B. Ganguly, A. Madhuram, D. Deshpande, J. Joshi, Biosorption of methyl violet, basic fuchsin and their mixture using dead fungal biomass, *Curr. Sci.*, 86 (2004) 1641–1645.
- [4] I.M. Banat, P. Nigam, D. Singh, R. Marchant, Microbial decolorization of textile dyes containing effluents: a review, *Bioresour. Technol.*, 58 (1996) 217–227.
- [5] J. Shore, Advances in direct dyes, *Indian J. Fib. Text. Res.*, 21 (1996) 1–29.
- [6] F. Nasiri Azad, M. Ghaedi, K. Dashtian, S. Hajati, A. Goudarzi, M. Jamshidi, Enhanced simultaneous removal of malachite green and safranin O by ZnO nanorod-loaded activated carbon: modeling, optimization and adsorption isotherms, *New J. Chem.*, 39 (2015) 7998–8005.
- [7] M. Dastkhooon, M. Ghaedi, A. Asfaram, A. Goudarzi, S.M. Langroodi, I. Tyagi, S. Agarwal, V.K. Gupta, Ultrasound assisted adsorption of malachite green dye onto ZnS:Cu-NPAC: equilibrium isotherms and kinetic studies – response surface optimization, *Separ. Purif. Technol.*, 156 (2015) 780–788.

- [8] E. Alipanahpour Dil, M. Ghaedi, A.M. Ghaedi, A. Asfaram, A. Goudarzi, S. Hajati, M. Soylak, S. Agarwal, V.K. Gupta, Modeling of quaternary dyes adsorption onto ZnO–NR–AC artificial neural network: analysis by derivative spectrophotometry, *J. Indust. Eng. Chem.*, 34 (2016) 186–197.
- [9] A. Asfaram, M. Ghaedi, S. Hajati, A. Goudarzi, Ternary dye adsorption onto MnO₂ nanoparticle-loaded activated carbon: derivative spectrophotometry and modelling, *RSC Adv.*, 5 (2015) 72300–72320.
- [10] M. Jamshidi, M. Ghaedi, K. Dashtian, S. Hajati, K. Dashidi, New ion-imprinted polymer-functionalized mesoporous SBA-15 for selective separation and preconcentration of Cr (iii) ions: modeling and optimization, *RSC Adv.*, 5 (2015) 105789–105799.
- [11] K.Y. Foo, B.H. Hameed, An overview of dye removal via activated carbon adsorption process, *Desal. Wat. Treat.*, 19 (2010) 255–274.
- [12] M.Y. Sobhy, S.A. Mahmoud, Removal of the hazardous crystal violet dye by adsorption on corncob-based and phosphoric acid-activated carbon, *Part. Sci. Technol.*, 33 (2015) 621–625.
- [13] T. Robinson, B. Chandran, P. Nigam, Removal of dyes from an artificial textile dye effluent by two agricultural waste residues, corncob and barley husk, *Environ. Int.*, 28 (2002) 29–33.
- [14] R.M. Gong, S.X. Zhu, D.M. Zhang, J. Chen, S.J. Ni, R. Guan, Adsorption behavior of cationic dyes on citric acid esterifying wheat straw: kinetic and thermodynamic profile, *Desalination*, 230 (2008) 220–228.
- [15] S.T. Ong, P.S. Keng, M.S. Voon, S.L. Lee, Application of durian peel (*Durio zibethinus* Murray) for the removal of methylene blue from aqueous solution, *Asian. J. Chem.*, 23 (2011) 2898–2902.
- [16] R. Han, D. Ding, Y. Xu, W. Zou, Y. Wang, Y. Li, L. Zou, Use of rice husk for the adsorption of Congo red from aqueous solution in column mode, *Bioresour. Technol.*, 99 (2008) 2938–2946.
- [17] F.D. Ardejani, K.H. Badii, N.Y. Limaee, N.M. Mahmoodi, M. Arami, S.Z. Shafaei, A.R. Mirhabibi, Numerical modelling and laboratory studies on the removal of Direct Red 23 and Direct Red 80 dyes from textile effluents using orange peel, a low-cost adsorbent, *Dyes Pigments*, 73 (2007) 178–185.
- [18] K. Vijayaraghavan, Y.-S. Yun, Bacterial biosorbents and biosorption, *Biotechnol. Adv.*, 26 (2008) 266–291.
- [19] S.K. Baskar, K. Pavithra, K.F. Sheraz, S. Renganathan, Optimization, equilibrium, kinetic modeling, and thermodynamic studies of biosorption of aniline blue by the dead biomass of *Aspergillus fumigatus*, *Desal. Wat. Treat.*, 52 (2014) 3547–3554.
- [20] V.A. Anagnostopoulos, B.D. Symeopoulos, Significance of age, temperature and aeration of yeast cell culture for the biosorption of europium from aquatic systems, *Desal. Wat. Treat.*, 15 (2016) 3957–3963.
- [21] M. Jerold, V. Sivasubramanian, Biosorption of malachite green from aqueous solution using brown marine macro algae *Sargassum swartzii*, *Desal. Wat. Treat.*, 57 (2016) 25288–25300.
- [22] E. Daneshvar, M. Kousha, M.S. Sohrabi, B. Panahbehagh, A. Bhatnagar, H. Younesi, S.P.K. Sternberg, Application of response surface methodology for the biosorption of Acid Blue 25 dye using raw and HCl-treated macroalgae, *Desal. Wat. Treat.*, 53 (2015) 1710–1723.
- [23] M. Kousha, E. Daneshvar, A.R. Esmaeili, H. Zilouei, K. Karimi, Biosorption of toxic acidic dye-Acid blue 25, by aquatic plants, *Desal. Wat. Treat.*, 52 (2014) 34–36.
- [24] J. Vijayaraghavan, T. Bhagavathi Pushpa, S.J. Sardhar Basha, K. Vijayaraghavan, J. Jegan, Evaluation of Red Marine Alga *Kappaphycus alvarezii* as biosorbent for methylene Blue: isotherm, kinetic, and mechanism studies, *Sep. Sci. Technol.*, 50 (2015) 1120–1126.
- [25] G.C. Panda, S.K. Das, A.K. Guha, Jute stick powder as a potential biomass for the removal of Congo Red and Rhodamine B from their aqueous solution, *J. Hazard. Mater.*, 164 (2009) 374–379.
- [26] H.P. Boehm, Some aspects of the surface chemistry of carbon blacks and other carbons, *Carbon*, 32 (1994) 759–769.
- [27] H. Mazaheri, M. Ghaedi, S. Hajati, K. Dashtian, M.K. Purkait, Simultaneous removal of methylene blue and Pb²⁺ ions using ruthenium nanoparticle-loaded activated carbon: response surface methodology, *RSC Adv.*, 5 (2015) 83427–83435.
- [28] T. Santhi, T. Manonmani, S. Smitha, Removal of malachite green from aqueous solution by activated carbon prepared from the epicarp of *Ricinus communis* by adsorption, *J. Hazard. Mater.*, 179 (2010) 178–186.
- [29] F.N. Azad, M.K. Dashtian, S. Hajati, A. Goudarzi, M. Jamshidi, Enhanced simultaneous removal of malachite green and safranine O by ZnO nanorod-loaded activated carbon: modeling, optimization and adsorption isotherms, *New J. of Chem.*, 39 (2015) 7998–8005.
- [30] Z. Bekci, Y. Seki, Y.L. Cavasb, Removal of malachite green by using an invasive marine alga *Caulerpa racemosa* var. *cylindracea*, *J. Hazard. Mater.*, 161 (2009) 1454–1460.
- [31] V. Murphy, H. Hughes, P. McLoughlin, Cu (II) binding by dried biomass of red, green and brown macroalgae, *Water Res.*, 41 (2007) 731–740.
- [32] O.S. Bello, M.A. Ahmad, B. Semire, Scavenging malachite green dye from aqueous solutions using pomelo (*Citrus grandis*) peels: kinetic, equilibrium and thermodynamic studies, *Desal. Wat. Treat.*, 56 (2015) 521–535.
- [33] A. Asfaram, M. Ghaedi, A. Goudarzi, M. Rajabi, Response surface methodology approach for optimization of simultaneous dye and metal ion ultrasound-assisted adsorption onto Mn doped Fe₃O₄-NPs loaded on AC: kinetic and isothermal studies, *Dalton Trans.*, 44 (2015) 14707–14723.
- [34] K.V. Kumar, V. Ramamurthi, S. Sivanesan, Modeling the mechanism involved during the sorption of methylene blue onto fly ash, *J. Colloid Interf. Sci.*, 284 (2005) 14–21.
- [35] G.C. Donmez, Z. Aksu, A. Ozturk, T.A. Kutsal, Comparative study on heavy metal biosorption characteristics of some algae, *Proc. Biochem.*, 34 (1999) 885–892.
- [36] S. Aksu, S. Tezer, Equilibrium and kinetic modeling of biosorption of Remazol Black B by *Rhizopus arrhizus* in a batch system: effect of temperature, *Proc. Biochem.*, 36 (2000) 431–439.
- [37] I.D. Mall, V.C. Srivastava, N.K. Agarwa, I.M. Mish, Adsorptive removal of malachite green dye from aqueous solution by bagasse fly ash and activated carbon – kinetic study and equilibrium isotherm analyses, *Colloids Surf. A.*, 264 (2005) 17–28.
- [38] M. Jamshidi, M. Ghaedi, K. Dashtian, S. Hajati, K. Dashtian, New ion-imprinted polymer-functionalized mesoporous SBA-15 for selective separation and preconcentration of Cr (iii) ions: modeling and optimization, *RSC Adv.*, 5 (2015) 105789–105799.
- [39] S. Dashamiri, M. Ghaedi, K. Dashtian, M.R. Rahimi, A. Goudarzi, R. Jannesar, Ultrasonic enhancement of the simultaneous removal of quaternary toxic organic dyes by CuO nanoparticles loaded on activated carbon: central composite design, kinetic and isotherm study, *Ultrason. Sonochem.*, 31 (2016) 546–557.
- [40] I. Langmuir, The adsorption of gases on plan surfaces of glass, mica and platinum, *J. Am. Chem. Soc.*, 40 (1918) 1361–1403.
- [41] K.R. Hall, L.C. Eagleton, A. Acrivos, T. Vermeulen, Pore- and solid-diffusion kinetics in fixed-bed adsorption under constant-pattern conditions, *Ind. Eng. Chem. Fundam.*, 5 (1966) 212–223.
- [42] H. Freundlich, Ueber die adsorption in loesungen, *Zeitschrift für Physikalische Chemie.*, 57 (1907) 385–470.
- [43] M.J. Temkin, V. Pyzhev, Recent modifications to Langmuir isotherms, *Acta Physiochim. USSR*, 12 (1940) 217–222.
- [44] R. Ahmad, R. Kumar, Adsorption studies of hazardous malachite green onto treated ginger waste, *J. Environ. Manage.*, 91 (2010) 1032–1038.
- [45] R. Rajesh Kannan, M. Rajasimman, N. Rajamohan, B. Sivaprakash, Brown marine algae *Turbinaria Conoides* as biosorbent for Malachite green removal: equilibrium and kinetic modeling, *Front. Environ. Sci. Engin. China*, 4 (2010) 116–122.
- [46] B.H. Hameed, M.I. El-Khaiari, Malachite green adsorption by rattan sawdust: isotherm, kinetic and mechanism modelling, *J. Hazard. Mater.*, 159 (2008) 574–579.
- [47] K.V. Kumar, Optimum sorption isotherm by linear and non-linear methods for malachite green onto lemon peel, *Dyes Pigments*, 74 (2007) 595–597.

- [48] Z. Bekci, Y. Seki, L. Cavas, Removal of malachite green by using an invasive marine alga *Caulerpa racemosa* var. *cylindracea*, *J. Hazard. Mater.*, 161 (2009) 1454–1460.
- [49] P.T. Godbole, A.D. Sawant, Removal of malachite green from aqueous solutions using immobilized *Saccharomyces cerevisiae*, *J. Sci. Ind. Res.*, 65 (2006) 440.
- [50] J. Zhang, Y. Li, C. Zhang, Y. Jing, Adsorption of malachite green from aqueous solution onto carbon prepared from *Arundo donax* root, *J. Hazard. Mater.*, 150 (2008) 774–782.
- [51] P. Saha, S. Chowdhury, S. Gupta, I. Kumar, R. Kumar, Assessment on the removal of malachite green using tamarind fruit shell as biosorbent, *Clean Soil Air Water*, 38 (2010) 437–445.
- [52] M. Ghaedi, H. Zare Khafri, A. Asfaram, A. Goudarzi, Response surface methodology approach for optimization of adsorption of Janus Green B from aqueous solution onto ZnO/Zn(OH)₂-NP-AC: kinetic and isotherm study, *Spectrochim. Acta Part A: Molec. Biomolec. Spectroscopy*, 152 (2016) 233–240.
- [53] A. Asfaram, M. Ghaedi, S. Hajati, A. Goudarzi, A.A. Bazrafshan, Simultaneous ultrasound-assisted ternary adsorption of dyes onto copper-doped zinc sulfide nanoparticles loaded on activated carbon: optimization by response surface methodology, *Spectrochim. Acta Part A: Molec. Biomolec. Spectroscopy*, 145 (2015) 203–212.
- [54] S. Langergren B.K. Svenska, Zur theorie der sogenannten adsorption geloster stoffe, *Veternskapsakad Handl.*, 24 (1898) 1–39.
- [55] G. McKay, Y.S. Ho, The sorption of lead (II) on peat, *Water Res.*, 33 (1999) 578–84.
- [56] G. McKay, Y.S. Ho, Pseudo-second-order model for sorption processes, *Proc. Biochem.*, 34 (1999) 451–465.
- [57] W.J. Weber, J.C. Morris, Proceedings of the International Conference on Water Pollution Symposium, Vol. 2, Pergamon, Oxford, 1962, pp. 231–266.
- [58] K.R. Hall, L.C. Eagleton, A. Acrivers, T. Vermenlem, Pore and solid diffusion and kinetics in fixed adsorption constant pattern conditions, *Ind. Eng. Chem. Res.*, 5 (1966) 212–223.
- [59] K.V. Kumar, A. Kumaran, Removal of methylene blue by mango seed kernel powder, *Biochem. Eng. J.*, 27 (2005) 83–93.